An Efficient Algorithmic Approach for the Estimation of the Red Edge Position of Plant Leaf Reflectance

Gladimir V.G. Baranoski * J.G. Rokne †

Technical Report CS-2002-29 - August 2002

Abstract. The point of maximum slope on the reflectance spectrum of vegetation between red and near-infrared wavelengths is known as the *red edge position (REP)*. The *REP* is strongly correlated with foliar chlorophyll content, and hence, it provides a very sensitive indicator for a variety of environmental factors such as vegetation stress, drought and senescence. Due to its importance for the application of inversion procedures, a number of techniques have been developed for determining the *REP* for foliar spectral reflectance. In this paper a new approach is proposed. It allows an unsupervised estimation of the *REP*. The accuracy of the new approach is evaluated by comparing *REP* estimates with values derived from measured spectral data for woody and herbaceous species.

1 Introduction

The abrupt reflectance change in the 680-770nm region of vegetation spectra caused by the combined effects of strong chlorophyll absorption and leaf internal scattering is called the *red edge*. As stated by Horler *et al.* [11], the existence of the red edge, although it is not measured directly, provides the basis for vegetation identification procedures using combinations of red and infrared radiances. A typical plant leaf reflectance spectrum is shown in

*School of Computer Science, University of Waterloo, Waterloo, Ontario, Canada

†Department of Computer Science, The University of Calgary, Calgary, Alberta, Canada

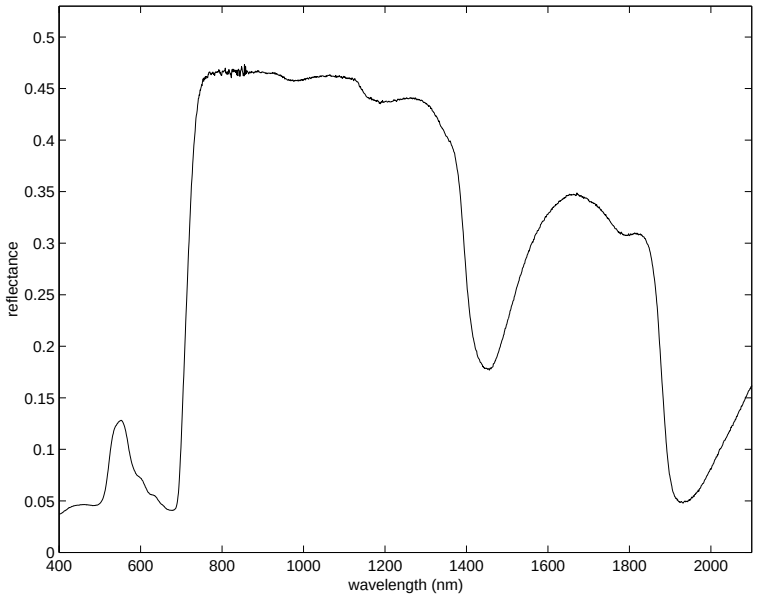

Figure 1: Spectral reflectance of soy *Soja hispida* [12].

Figure 1. The point of maximum slope on the red edge is called the *red edge position*, abbreviated the *REP*.

Chlorophyll concentration is usually an indicator of nutritional stress, photosynthetic capacity and senescence. It turns out that the position of the *REP* and the chlorophyll concentration is strongly correlated. Other constituents of plants such as amaranthin have also been shown to have functional relationships to the red edge [4].

Experiments by Danson and Plummer [5] have shown a strong non-linear correlation between leaf area index (*LAI*), the one-sided area of leaves per unit of ground area, and the *REP*. The *LAI* is a key spatial variable require to drive models of forest ecosystems [14], since it provides a quantitative measure of the surface area available for interception of photosynthetically active radiation (*PAR*) and transpiration.

The estimation of the *REP*, usually applying numerical methods for generating derivatives for leaf reflectance spectra, is, therefore, a valuable remote sensing tool to assess the chemical and morphological status of plants [2].In addition, the use of derivative spectrophotometry is commonly employed to resolve or enhance absorption features that might be masked by interfering background absorption [7, 8].

A number of methods for determining the *REP* have, therefore, been proposed in the remote sensing literature.

1. The simplest method is based on linear interpolation. It assumes the reflectance red edge can be simplified to a straight line centred around a midpoint between the shoulder reflectance maximum and the reflectance minimum of the chlorophyll reflectance curve, which is set usually at about $680nm$. The *REP* is then estimated by a simple linear equation using the slope of the line [9, 5].

2. The inverted Gaussian technique [1] assumes that the data can be fitted by a curve of the form

$$\rho(\lambda) = \rho_s - (\rho_s - \rho_0)e^{\frac{(\lambda-\lambda_0)^2}{2\sigma^2}} \tag{1}$$

   where $\rho(\lambda)$ is the reflectance as a function of the wavelength λ, ρ_0 is the reflectance where $\lambda = \lambda_0$ - usually around $680nm$, ρ_s is the "shoulder reflectance" - frequently set to $800nm$ and σ the gaussian shape parameter. The *REP* is then the inflection point of the curve at $\lambda_p = \sigma + \lambda_0$. A non-linear equation system would have to be solved in order to find a least-square fit to (1). Several of the constants are, therefore, estimated in [1] so that the resulting equation can be linearized to a linear least-squares system, which can be solved easily. The model was extensively tested and evaluated in [13]. The results are as good as the quality of the picked constants.

3. A three-point Lagrange interpolation technique of the derivative of the spectral data was given in [6]. A finite difference approximation is applied to four datapoints of $\rho(\lambda)$ to generate derivative approximations $D(\lambda_i),\ i = 1, 2, 3$. Then coefficients

$$A(\lambda_i) = \frac{D(\lambda_i)}{\prod_{i\neq j, j=1}^{3}(\lambda_i - \lambda_j)} \quad i = 1, 2, 3$$

   are calculated. These coefficients are used to calculate

$$REP = \frac{A(\lambda_1)(\lambda_2 - \lambda_3) + A(\lambda_2)(\lambda_1 - \lambda_3) + A(\lambda_3)(\lambda_1 - \lambda_2)}{2\sum_{i=1}^{3} A(\lambda_i)}$$

   The method is simple, but dependent on the quality of the location of the spectral sampling points as well as the spectral samples. It assumes that the derivative curve is a parabola.

4. Another technique locates the *REP* as the maximum first derivative of the reflectance spectrum in the region of the red edge using high-order curve fitting techniques to fit a continuous function to the derivative spectrum (see for example [11, 7, 16]).

Methods 1-3 above are compared by Dawson and Curran [6] taking into account different chlorophyll concentrations. It is noted that the red edge position at 50 $mg\ m^{-2}$ concentration is $705nm$ for the Lagrangian, $707nm$ for the inverse Gaussian and $715nm$ for the linear interpolation. These differences cast some doubt as to where the actual red edge position is located. Furthermore, the red edge position for the linear method at 50 $mg\ m^{-2}$ chlorophyll concentration is exactly the same as the red edge position for both the Lagrangian and the inverse Gaussian methods at 350 $mg\ m^{-2}$ chlorophyll concentration.

A different issue is highlighted by Pierce [15] in the description of REDR(1.0) (Red Edge Detection Engine), which is an application designed to detect the spectra that correspond to vegetation in multi- and hyper-spectral image datasets, and to compute a red edge location. Pierce distinguishes between supervised and unsupervised computations. The former is a computation supervised by a human expert. The later is a computation done automatically, *i.e.*, it seeks to achieve reasonably accurate results without the intervention of an expert. Pierce argues that the methods in the literature are satisfactory for supervised, but not for unsupervised computations for the *REP*. These remarks beg the questions of what exactly is the red edge, how can it be computed, how can the results be reproducible and to what accuracy can the results be trusted.

The aim of the present work is to first abstract the essential features of the reflectance spectrum which determine the red-edge position so that the red edge is as uniquely defined as possible. The results of a red edge position should also be reproducible, that is, given data on the spectrum two computations should give the same result. Also, the computation of the red edge should be unsupervised without introducing undue complexity. Finally, the evaluation of the technique used to estimate the *REP* should be based on comparisons with values derived from measured data, so that one can assess its usefulness to remote sensing applications.

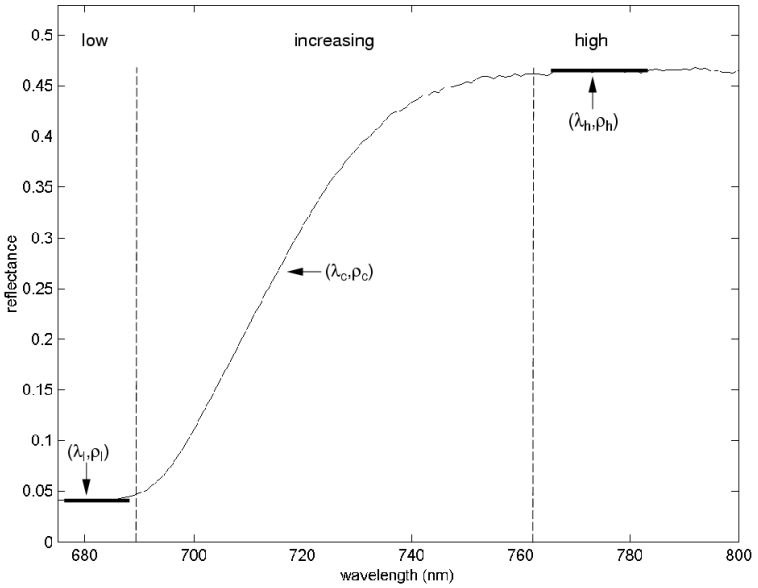

Figure 2: Regions in the reflectance spectrum of a soy (*Soja hispida*) leaf [12].

2 The Proposed Approach

Railyan and Korobov [16] acknowledged that the origin and behavior of the red edge is not described and explained completely. In fact one can find slightly different ranges for the red edge in the remote sensing literature. Most works in this area consider the lower bound to be $680nm$, while values for the upper bound vary from 740 to $800nm$.

If we consider the graph in Figure 2, we note that there are essentially three regions of reflectance in the general spectral region of the red edge. Initially, there is a region of low and relatively constant reflectance ρ_l, followed by a rapidly rising reflectance curve, which corresponds to the site of the red edge. Finally, we observe a region of high and relatively constant reflectance ρ_h.

Our goal here is to abstract these features by a new function:

$$f(x) = \frac{a + bx + cx^2}{1 + dx + ex^2} \tag{2}$$

of five parameters that will encompass the features mentioned above. Four

of the conditions determining the parameters are

$$\begin{aligned} f(\lambda_l) &= \rho_l && (3)\\ f'(\lambda_l) &= 0 && (4)\\ f(\lambda_h) &= \rho_h && (5)\\ f'(\lambda_h) &= 0 && (6) \end{aligned}$$

which requires a decision on the locations of (λ_l, ρ_l) and (λ_h, ρ_h). The remaining condition is that a point (λ_c, ρ_c) in the red-edge region be chosen from the data.

These five equations result in a mildly non-linear 5×5 system of equations. Although it is possible to solve this system directly, it is simpler to shift the coordinate system with a linear transformation, so that the origin is given by the pair (λ_l, ρ_l), and the upper point of the curve is given by the pair (W, R), where $W = \lambda_h - \lambda_l$ and $R = \rho_h - \rho_l$. A function

$$g(x) = \frac{A + Bx + Cx^2}{1 + Dx + Ex^2} \tag{7}$$

is then considered and equations (3)-(6) are replaced by

$$\begin{aligned} g(0) &= 0 && (8)\\ g'(0) &= 0 && (9)\\ g(W) &= R && (10)\\ g'(W) &= 0. && (11) \end{aligned}$$

To solve these equations we first consider $g(0) = 0$ which results in $A = 0$. From $g'(0) = 0$ we get $B = 0$.

Now $g(W) = R$ results in

$$R = \frac{CW^2}{1 + DW + EW^2} \tag{12}$$

and $g'(W) = 0$ gives

$$2CW(1 + DW + EW^2) = (D + 2EW)CW^2. \tag{13}$$

These two equations can be simplified to

$$\begin{aligned} DRW + ERW^2 &= CW^2 - R, && (14)\\ DR + 2EWR &= 2CW. && (15) \end{aligned}$$

Using Cramer's rule we get

$$D = -2/W, \tag{16}$$

$$E = C/R + 1/W^2 \tag{17}$$

which determines D and E in terms of a parameter C. Equation (7) can now be written as

$$g(x) = \frac{Cx^2}{1 - 2x/W + (\frac{C}{R} + \frac{1}{W^2})x^2}. \tag{18}$$

The point (ρ_c, λ_c) on the ascending part of the curve is also translated to a point (λ_c', ρ_c') in the shifted coordinate system and used to determine C as

$$C = \frac{(1/\lambda_c' - 1/W)^2}{1/\rho_c' - 1/R} \tag{19}$$

Let now

$$g(x) = \frac{Cx^2}{1 + Dx + Ex^2}. \tag{20}$$

where C, D, E are defined by Equations (19), (16), (17) respectively. The first derivative is given by:

$$g'(x) = \frac{Cx(2 + Dx)}{(1 + Dx + Ex^2)^2} \tag{21}$$

and the second derivative is given by:

$$g''(x) = \frac{-2C(-1 + Ex^2(3 + Dx))}{(1 + Dx + Ex^2)^3}. \tag{22}$$

Finally, we set $g''(x) = 0$ and solve for x. This equation has three roots, one of which is in the interval $[0, W]$ of interest. Using the auxiliary quantity

$$P = ((D^2 - 2E)E^2 + \sqrt{D^2E^4(D^2 - 4E)})^{1/3}/E \tag{23}$$

we get

$$x = \frac{1}{D}\left(-\frac{(1 - i\sqrt{3})}{2^{2/3}P} - \frac{P(1 + i\sqrt{3})}{2^{4/3}} - 1\right) \tag{24}$$

and $REP = x + \lambda_l$.

In general we can write down an algorithm for the estimation of the REP as follows:

FindREP

1. Input (λ_l, ρ_l), (λ_h, ρ_h), (λ_c, ρ_c).
2. Compute

$$\begin{aligned} W &= \lambda_h - \rho_l, \\ R &= \rho_h - \rho_l, \\ \lambda_c' &= \lambda_c - \lambda_l, \\ \rho_c' &= \rho_c - \rho_l. \end{aligned}$$

3. Calculate D using Equation (16).
4. Calculate E using Equation (17).
5. Calculate C using Equation (19).
6. Solve for x in the equation $g''(x) = 0$ in $[0, W]$ using Equations (23) and (24).
7. $REP = x_+ \lambda_l$.

3 Evaluation

3.1 Data and Methods

In our evaluation of the proposed approach we compare estimated red edge curves with spectral curves originated from measured data. More specifically, in our experiments we consider specimens whose reflectance spectra are available in the LOPEX (Leaf Optical Properties Experiment) [12] database. This database consists of 70 leaf samples representing 50 woody and herbaceous species that were obtained from trees and crops near the Joint Research Centre in Ispra, Italy. Reflectance spectra were originally scanned in $1 - 2nm$ steps, but the wavelength interval was averaged over $5nm$ to reduce noise. The derivate for these curves were computed using a three-point numerical differentiation formula [3]. We also applied a local average smoothing to reduce noise.

The estimated red edge curves are plotted using the following algorithm:

PlotRED

1. Input (λ_l, ρ_l), (λ_h, ρ_h), (λ_c, ρ_c).
2. Compute

$$\begin{aligned} W &= \lambda_h - \rho_l, \\ R &= \rho_h - \rho_l, \\ \lambda_c' &= \lambda_c - \lambda_l, \\ \rho_c' &= \rho_c - \rho_l. \end{aligned}$$

3. Calculate D using Equation (16).
4. Calculate E using Equation (17).
5. Calculate C using Equation (19).
6. Plot estimated red edge, $g(\lambda)$, using Equation (20) shifted in wavelength axis according to λ_l.
7. Plot derivative of the estimated red edge, $g'(\lambda)$, using Equation (21).

The accuracy of *REP* locating procedures is sensitive to the red egde bounds used as input parameters. Supervised approaches usually tailor the choice of sample wavelengths to the specimen at hand. Unsupervised approaches, like the one proposed in this paper, use fixed values for these parameters. As mentioned earlier, one can find slightly different values for these bounds in the literature. In our experiments we use $\lambda_l = 680nm$ and $\lambda_h = 770nm$. An optimal choice for a point in the red edge would be given by $\rho_c = REP$. Clearly this is not an option. since if we already knew the *REP*, we would not need to estimate it! Therefore, we simply use $\lambda_c = (\lambda_l + \lambda_h)/2 = 725nm$ in our estimations.

In order to perform a comprehensive validation of a *REP* estimation method it would be necessary to consider a large number of specimens. For practical reasons, in our comparisons we considered six specimens representing herbaceous and woody species: maize (*Zea mays L.*), iris (*Iris germanica*

L.), poplar (*Populus canadensis*), soy (*Soja hispida*), maple (*Acer pseudo-platanus L.*) and tomato (*Lycopersicum esculentum*). Table 1 presents the specimens' reflectances (ρ_l, ρ_c and ρ_h)sampled from LOPEX measured data and used in our estimations.

Specimen	ρ_l	ρ_c	ρ_h
maize	0.0648	0.2839	0.4657
iris	0.0331	0.3749	0.4916
poplar	0.0627	0.3189	0.4691
soy	0.0410	0.3464	0.4655
maple	0.0382	0.2870	0.4126
tomato	0.0452	0.3215	0.4399

Table 1: Reflectance values for the six specimens at the specified wavelengths: $\lambda_l = 680nm$, $\lambda_c = 725nm$ and $\lambda_h = 780nm$. Source: LOPEX [12].

3.2 Results

Figures 3 and 8 present comparisons between red edge and derivative curves plotted using **PlotRED** and curves derived from LOPEX reflectance data. A visual inspection of these plots suggests a good agreement between the estimated and measured reflectance curves.

While the estimated derivative curves present good qualitative agreement with the derivative curves determined from measured data, quantitative discrepancies are noticeable, especially for some of the species considered, namely maize (Figure 3) and maple (Figure 7). The inflection points of the curves are, however, fairly close, suggesting that the proposed approach for the estimation of *REP* presents an acceptable level of accuracy.

Table 2 presents the *REP* values derived from the measured reflectance spectrum of each specimen considered, and values estimated using **FindREP**. For all specimens considered the relative error is smaller than 1%, and for four of the specimens tested it is smaller than 0.3%. These figures confirm the observations derived from the visual inspection of the derivative curves, *i.e.*, the estimated *REP* values closely approximate the actual values for the tested specimens.

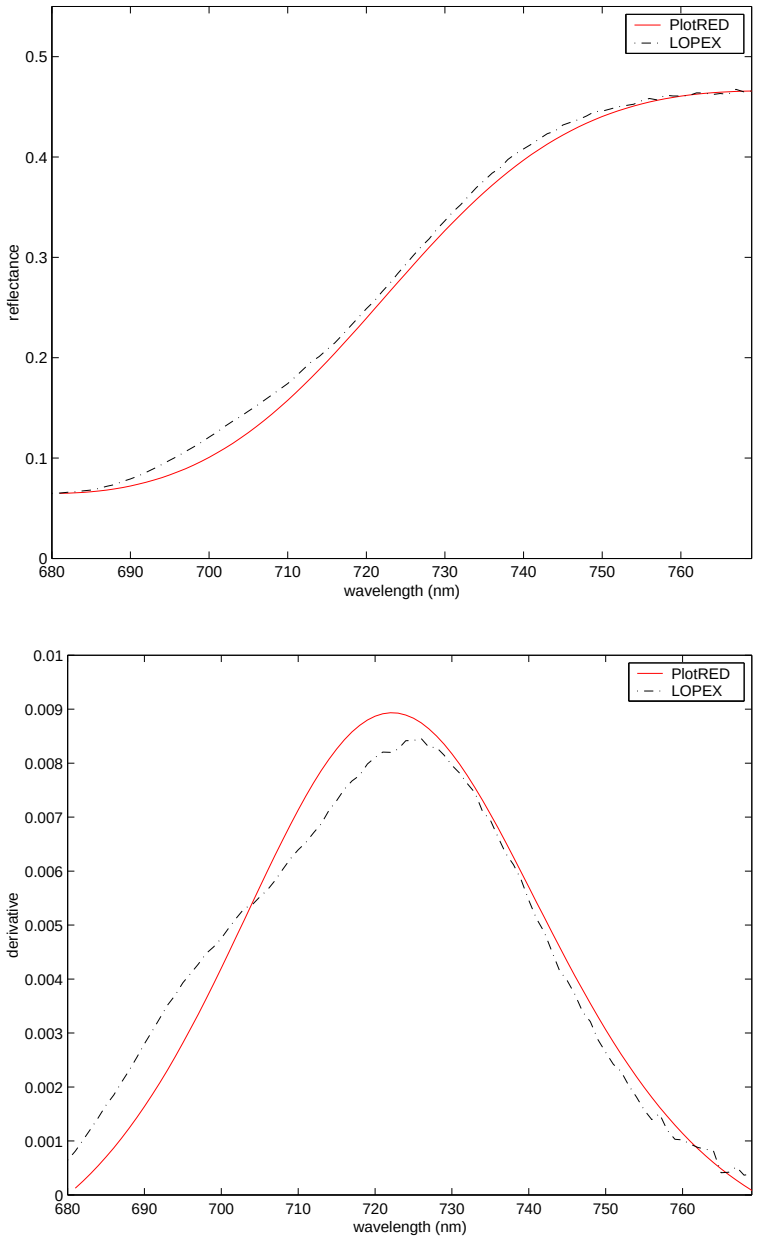

Figure 3: Estimated (PlotRED) and measured (LOPEX) reflectance and first derivative curves for maize (*Zea mays L.*).

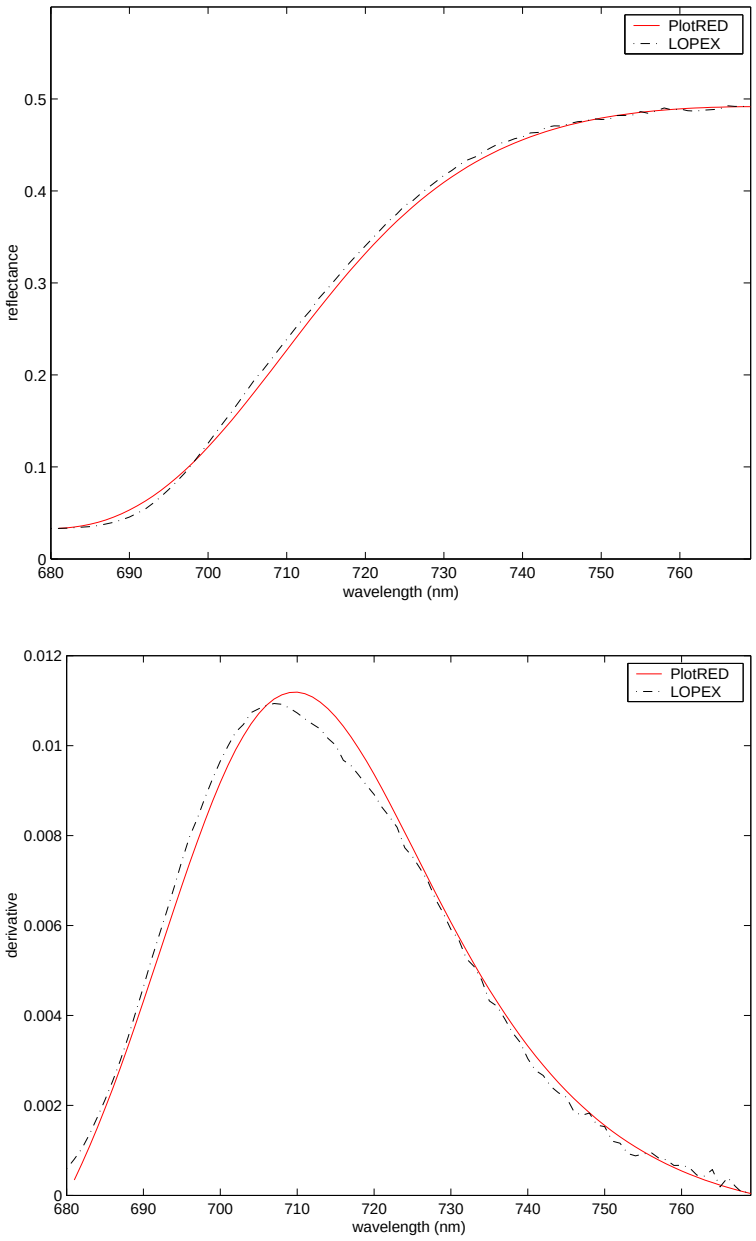

Figure 4: Estimated (PlotRED) and measured (LOPEX) reflectance and first derivative curves for iris (*Iris germanica L.*).

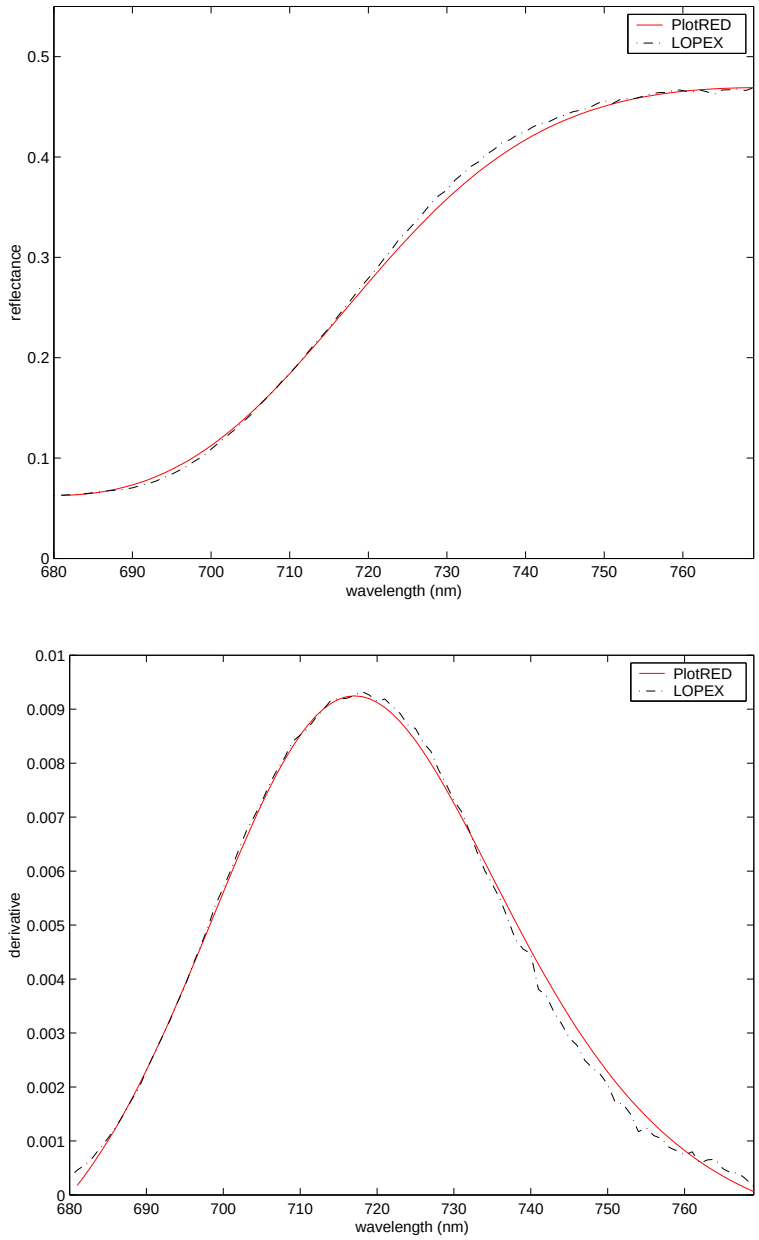

Figure 5: Estimated (PlotRED) and measured (LOPEX) reflectance and first derivative curves for poplar (*Populus canadensis*).

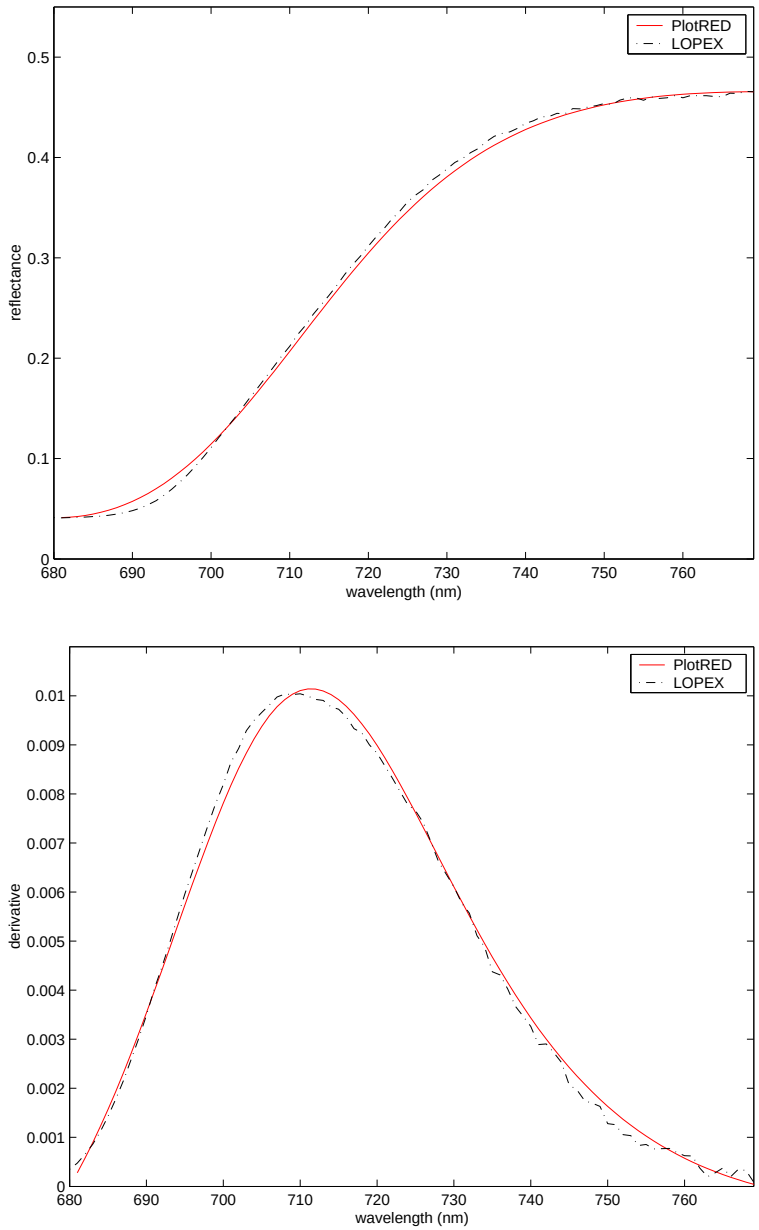

Figure 6: Estimated (PlotRED) and measured (LOPEX) reflectance and first derivative curves for soy (*Soja hispida*).

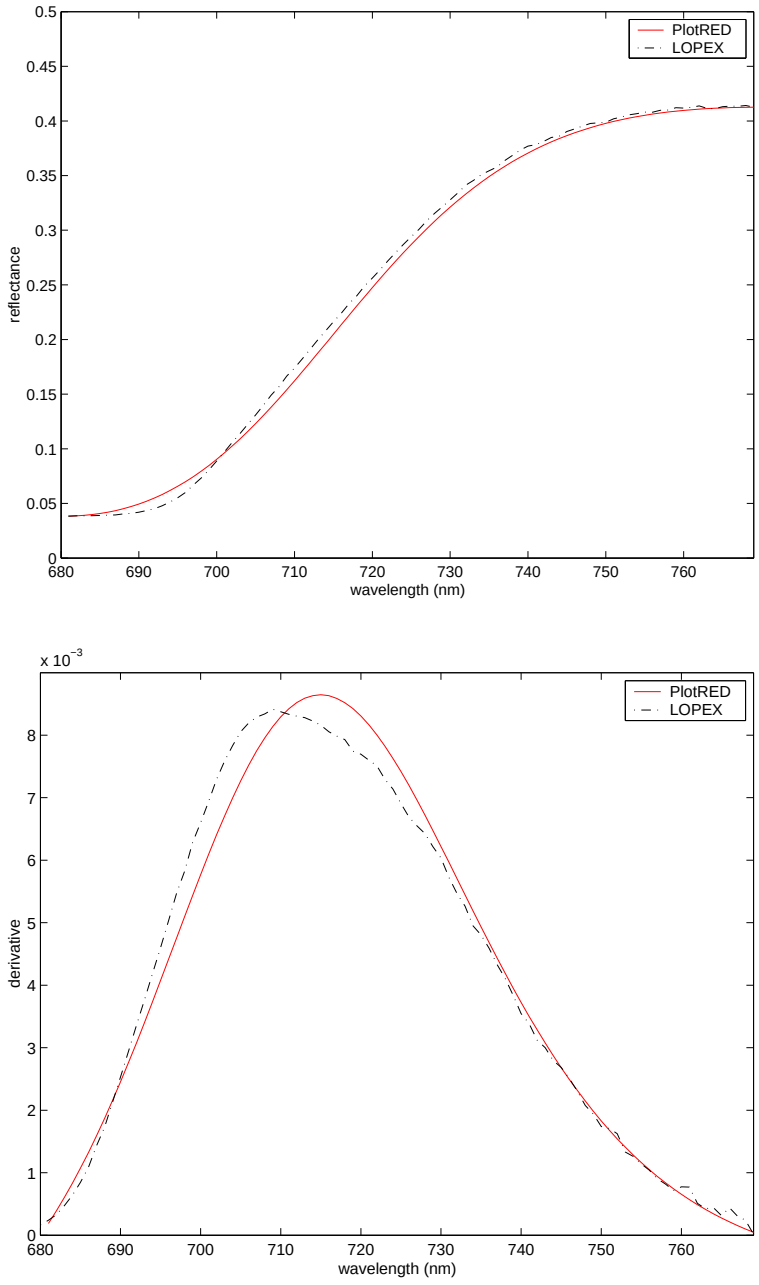

Figure 7: Estimated (PlotRED) and measured (LOPEX) reflectance and first derivative curves for maple (*Acer pseudoplatanus L.*).

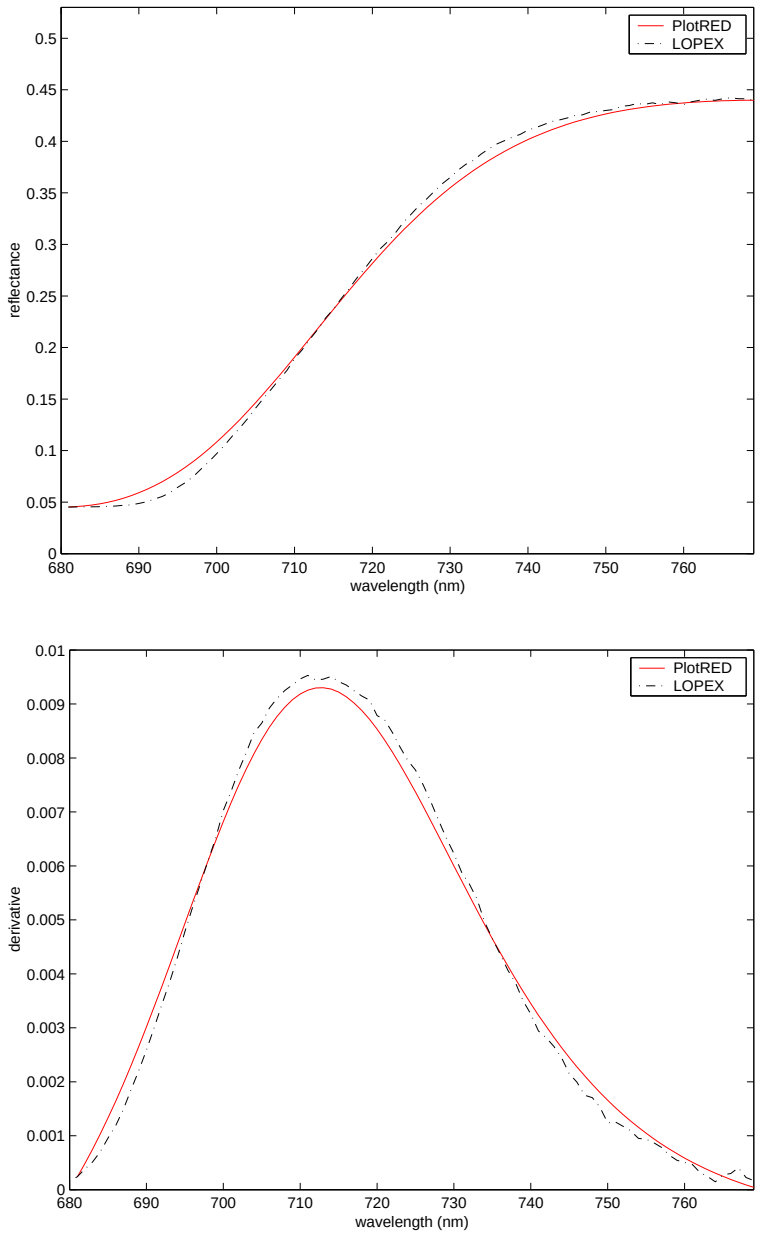

Figure 8: Estimated (PlotRED) and measured (LOPEX) reflectance and first derivative curves for tomato (*Lycopersicum esculentum*).

Specimen	Red Edge Position		Relative Error
	LOPEX	FindREP	
maize	$727nm$	$722.20nm$	0.66%
iris	$708nm$	$709.67nm$	0.24%
poplar	$719nm$	$717.09nm$	0.29%
soy	$711nm$	$711.42nm$	0.06%
maple	$710nm$	$714.96nm$	0.70%
tomato	$712nm$	$712.68nm$	0.10%

Table 2: Comparison between measured (LOPEX) and estimated (FindREP) red edge positions for different plants leaves.

4 Discussion

The proposed approach for the estimation of the *REP* assumes no *a priori* knowledge about the reflectance spectrum of a given specimen. As previous techniques used to estimate the *REP*, it may be affected by the choice of input parameters, namely the three wavelength sample positions (λ_l, λ_c and λ_h). Instead of supervising the choice of these values for each specimen, fixed values ($680nm$, $725nm$ and $770nm$ respectively) were used in the evaluation experiments. As a result the relative errors fluctuate, but their magnitudes remain within reasonable limits, especially considering that the comparisons are performed with respect to values derived from actual measured data, instead of values estimated by other techniques.

The analytical solution provided by the proposed approach has the property that the complex parts cancel out if the arithmetic is exact. Floating point arithmetic, however, is not exact. As a result, an estimation may have tiny complex parts, in the order of 10^{-14}, which should be discarded. Alternatively, instead of using the closed formulas given by Equations (23) and (24), one could apply a numerical root finding procedure, such as `fzero` in Matlab [10], or an equivalent in any other numerical software package, with Equation (22) as the target function.

Selecting the "best" *REP* estimation method is delicate, and no single method is superior in all the cases. The relative accuracy depends on the biological characteristics of the specimen at hand. Furthermore, the evaluation of a computer method is less predictable than measuring physical phenom-

ena. Nonetheless, our experiments suggest that the proposed algorithmic approach provides *REP* estimates with reasonably high accuracy/cost ratio, without requiring human intervention. Hence, it may be suitable for the estimation and analysis of red edge data in field, laboratory, airborne and spaceborne settings. Our future efforts will be focus on the application of the proposed approach to estimate *REP* shifts due natural seasonal cycles affecting the concentration of chlorophyll.

References

[1] G.F. Bonham-Carter. Numerical procedures and computer program for fitting an inverted gaussian model to vegetation reflectance data. *Computers and Geosciences*, 14:339–356, 1988.

[2] F. Boochs, G. Kupfer, K. Dockter, and W. Kuhbauch. Shape of the red edge as vitality indicator for plants. *International Journal of Remote Sensing*, 11:1741–1753, 1990.

[3] R.L. Burden and J.D. Faires. *Numerical Analisys*. PWS Publishing Company, Boston, fifth edition, 1993.

[4] P.J. Curran, J.L. Dungan, B.A. Macler, and S. E. Plummer. The effect of a red leaf pigment on the relationship between red edge and chlorophyll concentration. *Remote Sensing of Environment*, 35:69–76, 1991.

[5] F.M. Danson and S.E. Plummer. Red edge response to forest leaf area index. *International Journal of Remote Sensing*, 16:183–188, 1995.

[6] T.P. Dawson and P.J. Curran. A new technique for interpolating the reflectance edge position. *International Journal of Remote Sensing*, 19:2133–2139, 1998.

[7] T.H. Demetriades-Shah, M.D. Steven, and J.A. Clark. High resolution derivative spectra in remote sensing. *Remote Sensing of Environment*, 33:55–64, 1990.

[8] I. Filella and J. Pe nuelas. The red edge position and shape as indicators of plant chlorophyll content, biomass and hydric status. *International Journal of Remote Sensing*, 15:1459–1470, 1994.

[9] G. Guyot, F. Baret, and S. Jacquemoud. Imaging spectroscopy for vegetation studies. In F. Toselli and J. Bodechtel, editors, *Imaging Spectrometry: Fundamentals and Prospective Applications*, pages 145–165, Dordrecht, 1992. Kluwer Academic.

[10] D. Hanselman and B. Littlefield. *Mastering MATLAB 6 A Comprehensive Tutorial and Reference.* Prentice Hall, Upper Saddle River, NJ, 2001.

[11] D.N.H. Horler, M. Dockray, and J. Barber. The red edge of plant leaf reflectance. *International Journal of Remote Sensing*, 4:273–288, 1983.

[12] B. Hosgood, S. Jacquemoud, G. Andreoli, J. Verdebout, G. Pedrini, and G. Schmuck. Leaf optical properties experiment 93. Technical Report Report EUR 16095 EN, Joint Research Center, European Comission, Institute for Remote Sensing Applications, 1995.

[13] J.R. Miller, E.W. Hare, and J. Wu. Quantitative characterisation of the vegetation red edge reflectance. 1. an inverted-gaussian reflectance model. *International Journal of Remote Sensing*, 11:1755–1773, 1990.

[14] R.R. Nemani, L.L. Pierce, S.W. Running, and L.E. Band. Forest ecosystem processes at the watershed scale: sensitivity to remotely-sensed leaf area index estimates.

[15] J. Pierce. Rede 1.0 (red edge detection engine). WWW document at: http://www.cstars.ucdavis.edu, 2002.

[16] V.Y. Railyan and R.M. Korobov. Red edge structure of canopy reflectance spectra of triticale. *Remote Sensing of Environment*, 46:173–182, 1993.